

$z \sim 7 - 10$ GALAXIES BEHIND LENSING CLUSTERS: CONTRAST WITH FIELD SEARCH RESULTS

RYCHARD J. BOUWENS², GARTH D. ILLINGWORTH², LARRY D. BRADLEY³, HOLLAND FORD³, MARIJN FRANX⁴, WEI ZHENG³, TOM BROADHURST⁵, DAN COE⁶, M. JAMES JEE⁷

¹ Based on observations made with the NASA/ESA Hubble Space Telescope, which is operated by the Association of Universities for Research in Astronomy, Inc., under NASA contract NAS 5-26555. These observations are associated with programs #5352, 5935, 6488, 8249, 8882, 9289, 9452, 9717, 10150, 10154, 10200, 10325, 10504, 10863, 10996.

² Astronomy Department, University of California, Santa Cruz, CA 95064

³ Department of Physics and Astronomy, Johns Hopkins University, 3400 North Charles Street, Baltimore, MD 21218

⁴ Sterrewacht Leiden, Leiden University, NL-2300 RA Leiden, Netherlands

⁵ School of Physics and Astronomy, Tel Aviv University, Tel Aviv 69978, Israel

⁶ Jet Propulsion Laboratory, California Institute of Technology, MS 169-327, Pasadena, CA 91109 and

⁷ Department of Physics, 1 Shields Avenue, University of California, Davis, CA 95616

Draft version February 10, 2022

ABSTRACT

We conduct a search for $z \gtrsim 7$ dropout galaxies behind 11 massive lensing clusters using 21 arcmin² of deep HST NICMOS, ACS, and WFPC2 image data. In total, over this entire area, we find only one robust $z \sim 7$ z -dropout candidate (previously reported around Abell 1689). Four less robust z -dropout and J -dropout candidates are also found. The nature of the four weaker candidates could not be precisely determined due to the limited depth of the available optical data, but detailed simulations suggest that all four could be low-redshift interlopers. We compare these numbers with what we might expect using the $z \sim 7$ UV luminosity function (LF) determined from field searches. We predict 2.7 $z \sim 7$ z -dropouts and 0.3 $z \sim 9$ J -dropouts over our cluster search area, in reasonable agreement with our observational results, given the small numbers. The number of $z \gtrsim 7$ candidates we find in the present search are much lower than has been reported in several previous studies of the prevalence of $z \gtrsim 7$ galaxies behind lensing clusters. To understand these differences, we examined $z \gtrsim 7$ candidates in other studies and conclude that only a small fraction are likely to be $z \gtrsim 7$ galaxies. Our findings support models that show that gravitational lensing from clusters is of the most value for detecting galaxies at magnitudes brighter than L^* ($H \lesssim 27$) where the LF is expected to be very steep. Use of these clusters to constrain the faint-end slope or determine the full LF is likely of less value due to the shallower effective slope measured for the LF at fainter magnitudes, as well as significant uncertainties introduced from modelling both the gravitational lensing and incompleteness.

Subject headings: galaxies: evolution — galaxies: high-redshift

1. INTRODUCTION

Because of the great distances and extreme faintness of galaxies at $z \gtrsim 7$, as well as the high sky backgrounds, detection of galaxies at such high redshifts remains extremely challenging. It is not surprising that the number of robust $z \gtrsim 7$ candidates is still very small (see, e.g., Bouwens & Illingworth 2006; Bouwens et al. 2008; Oesch et al. 2008). Gravitational lensing by galaxy clusters has been highlighted as an efficient way of improving this situation, due to the significant areas on the sky behind these clusters with sizeable magnification factors to amplify light from faint sources. However, this advantage is offset by the greatly reduced source plane volume in the highly magnified regions.

Because of the trade-off between depth and area, the utility of clusters for these searches depends strongly on the slope of the luminosity function (e.g., Broadhurst et al. 1995). If the effective slope of the LF ($-d(\log d\Phi)/d \log L$) is greater than 1, the gain in depth more than compensates for the loss in area, increasing the overall number of sources (e.g., Broadhurst et al. 1995) over that found in the field. Such steep slopes are found at magnitudes brighter than L^* (corresponding to $H \lesssim 27$ AB mag for $z \sim 7$ galaxies). By contrast, at fainter magnitudes ($H \gtrsim 27$ for $z \sim 7$ galaxies) the effective slope of the LF is not quite so steep (e.g., the

faint-end slope for the Bouwens et al. 2007 $z \sim 6$ LF corresponds to $-d(\log \Phi)/d(\log L) \sim 0.7 < 1$). This trade-off between depth and area is such that the surface density of dropouts is lower behind clusters than in the field at faint magnitudes. Overall these considerations suggest that the most significant advantages will be achieved at bright magnitudes ($>L^*$) where the LF is very steep. Shallow searches over many clusters, in particular, would seem to be the most rewarding.

Here we assess the promise of clusters for studying $z \gtrsim 7$ galaxies by conducting a careful search for high redshift galaxies in all the currently available HST NICMOS imaging data over 11 massive low-redshift galaxy clusters. Bradley et al. (2008) have already conducted such a search around Abell 1689 and reported one highly robust $z \gtrsim 7$ galaxy. Richard et al. (2006) examined 2 clusters and reported 13 $z \gtrsim 6$ candidates, while Richard et al. (2008) have examined 6 clusters and reported 12 $z \gtrsim 6$ candidates. The present paper represents an independent assessment of the prevalence of these sources behind massive low-redshift clusters. We take advantage of ~ 21 arcmin² of very deep NICMOS data behind 11 lensing clusters with optical ACS+WFPC2 coverage, 7 of which were already considered in the Bradley et al. (2008) and Richard et al. (2008) papers. For our $z \gtrsim 7$ search, we will utilize many of the same photometric techniques we have employed over the past few years

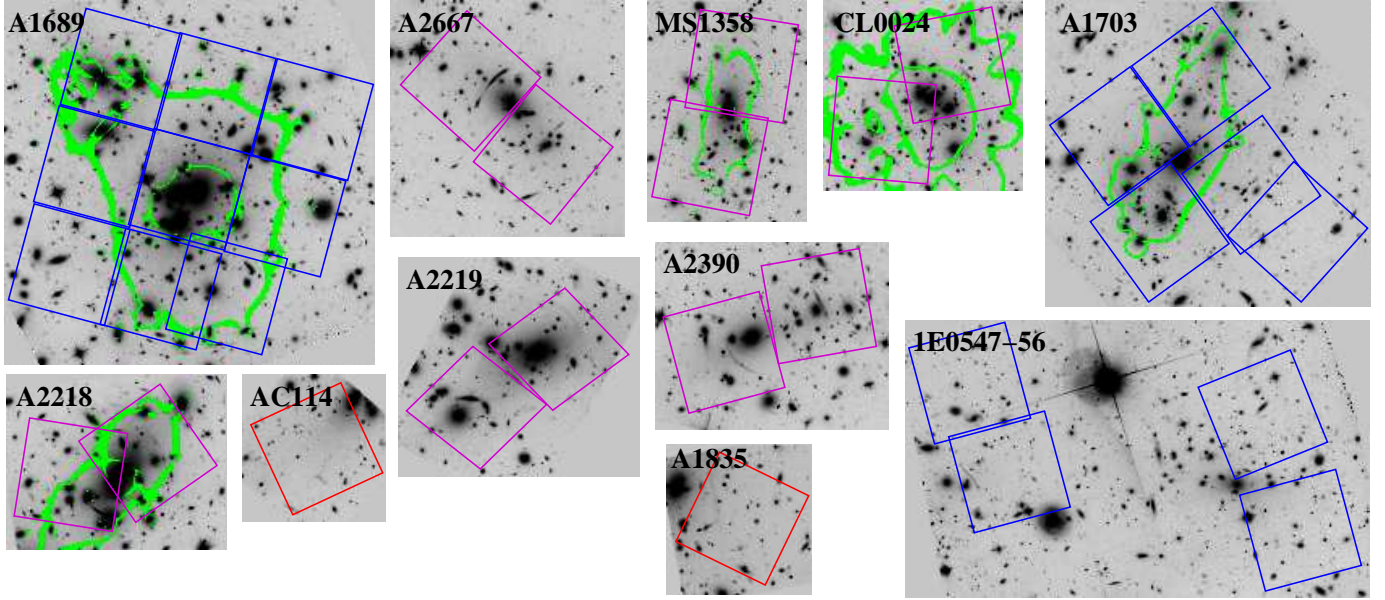


FIG. 1.— Optical ACS images of the 11 massive lensing clusters we used to search for star-forming galaxies at $z \gtrsim 7$. The name of each cluster is included in the upper left corner of the corresponding cluster image. Overlaid on these images are outlines of our deep NIC3 search fields, where magenta indicates that the field has deep (~ 3 -5 orbit) data in both the J_{110} and H_{160} bands, blue indicates the field only has shallow (~ 1 -2 orbit) data in the J_{110} band, and red indicates the field only has deep (~ 4 orbit) data in the H_{160} band (see Table 1). The green contours show the position of the critical curves at $z \sim 7$ (i.e., where the magnification $\mu > 100$) as determined from several published lensing models (Limousin et al. 2007; Limousin et al. 2008; Eliasdóttir et al. 2007; Jee et al. 2007; Franx et al. 1997).

TABLE 1
HST NICMOS DATA AROUND MASSIVE GALAXY CLUSTERS USED TO SEARCH
FOR $z \gtrsim 7$ GALAXIES.

Name	Area (arcmin ²)	Optical ^b	5 σ Depth ^a			NICMOS	
			z_{850}	J_{110}	H_{160}	orbits	Ref ^c
MS1358	1.4	28.0	27.5	26.8	26.7	18	[1]
CL0024	1.4	27.8	27.4	26.8	26.7	18	[1]
Abell 2218	1.2	27.9	27.6	26.8	26.7	17	[1]
Abell 2219	1.4	27.5	27.2	26.8	26.7	18	[1]
Abell 2390	1.5	26.6 ^d	26.9	26.8	26.7	18	[1]
Abell 2667	1.5	26.5 ^d	26.9	26.8	26.7	18	[1]
Abell 1689	5.7	28.1	26.8	26.4	—	19	[2]
Abell 1703	3.1	27.9	26.7	26.0	—	6	—
1E0657-56 ^e	2.7	27.6	27.2	26.0	—	4	—
Abell 1835	0.7	27.1 ^d	27.2	—	26.7	4	—
AC114	0.7	27.1 ^d	27.2	—	26.7	4	—
Total	21.3					144	

^a5 σ limits assume a 0.3''-diameter aperture for ACS/WFPC2 and 0.6''-diameter aperture for NICMOS.

^bThe depth of the deepest single-band optical ($\leq 0.8\mu$) image available over the cluster. Note that some of the clusters listed here have very deep data in ≥ 2 bands (particularly MS1358, CL0024, Abell 2218, Abell 1689, Abell 1703), so the effective depth of the combined optical data is often >0.4 mag deeper than tabulated here.

^cReferences: [1] Richard et al. 2008, [2] Bradley et al. 2008.

^dThe optical data available over these four clusters are from WFPC2 and are only moderately deep. As a result, we might expect a small number of low redshift interlopers to make it into $z \gtrsim 7$ selections (§4) conducted over each of these clusters. Not surprisingly, a substantial fraction of the weaker $z \gtrsim 7$ candidates in our own selection, and that of Richard et al. (2008) are found over these four clusters.

^eThe “Bullet” cluster

to identify large samples of $z \sim 4-8$ *BVi*z dropouts in the field (Bouwens et al. 2006; Bouwens et al. 2007; Bouwens et al. 2004; Bouwens et al. 2008).

We begin this paper with a summary of the observational data available to search for $z \gtrsim 7$ galaxies behind galaxy clusters (§2). In §3, we describe our techniques for constructing source catalogs and doing the photometry (§3). In §4, we summarize the results of our selection and discuss sources of contamination. In §5, we compare our results with (1) what we would expect based upon the $z \sim 7$ LF derived in the field and (2) the search results from other teams. We then conclude by discussing the implications of this study (§6). In the Appendix, we provide an assessment of the $z \gtrsim 7$ candidates reported by Richard et al. (2008). In particular, we assess the merits of searching for $z \gtrsim 7$ galaxies behind clusters versus searching for these galaxies in the field (§6). We assume $\Omega_0 = 0.3$, $\Omega_\Lambda = 0.7$, $H_0 = 70$ km/s/Mpc throughout. Although these parameters are slightly different from those determined from the WMAP five-year results (Dunkley et al. 2008), they allow for convenient comparison with other recent results expressed in a similar manner. The HST filters F555W, F606W, F625W, F702W, F775W, F814W, F850LP, F110W, and F160W will be denoted as V_{555} , V_{606} , r_{625} , R_{702} , i_{775} , I_{814} , z_{850} , J_{110} , and H_{160} , respectively. We will express all magnitudes in the AB system (Oke & Gunn 1983).

2. OBSERVATIONAL DATA

We conduct searches for dropout galaxies over the 11 low-redshift galaxy clusters with deep near-IR NICMOS and optical ACS coverage (Table 1). The near-IR data here were taken with the goal of finding $z \gtrsim 7$ galaxies. The NICMOS coverage of the first six clusters considered here (CL0024, MS1358, Abell 2218, Abell 2219, Abell 2390, Abell 2667) extends over 8.4 arcmin² (12 NIC3 pointings) and includes very deep imaging in both the J_{110} and H_{160} bands (Richard et al. 2008). The NICMOS coverage of three other clusters considered here (i.e., Abell 1689, Abell 1703, and 1E0657-56) is somewhat shallower in general, extends over ~ 10 arcmin² (17 NIC3 pointings), and is mainly in the J_{110} band. The final two clusters considered here (Abell 1835 and AC114) only have deep near-IR NICMOS data in the H_{160} band and over one ~ 0.8 arcmin² NIC3 pointing per cluster. The layout of our NICMOS search fields is illustrated graphically in Figure 1.

Deep optical imaging data are necessary for the selection of $z \gtrsim 7$ galaxies and can be a significant limitation, if not available. MS1358, CL0024, Abell 1689, Abell 1703, and Abell 2218 all possess useful optical data, with ≥ 2 orbits in each of the ACS g_{475} , r_{625} , and i_{775} bands and ≥ 6 orbits in the ACS z_{850} band. The optical coverage of Abell 2219, Abell 2390, Abell 2667, 1E0657-56, Abell 1835, and AC114 is generally shallower in depth and primarily with WFPC2, though ~ 4 orbits of ACS z -band coverage are available for each.

All the available ACS and NICMOS data over these clusters are processed into image mosaics using the ACS GTO pipeline “apsis” (Blakeslee et al. 2003) and NICMOS pipeline “nicred.py” (Magee et al. 2007). Reductions of the WFPC2 data are obtained from the Canadian Astronomy Data Centre. All reductions are registered onto the same frame as the NICMOS data.

3. SAMPLE CONSTRUCTION

(a) *Catalog Generation:* Our procedure for generating source catalogs and doing photometry is identical to that performed in Bouwens et al. (2008). Briefly, we run SEXtractor (Bertin & Arnouts 1996) in double-image mode to do object detection and photometry. For the detection image, we use the square root of the χ^2 image (Szalay et al. 1999), which we construct from the NICMOS J_{110} and H_{160} images for our z_{850} dropout selection and the NICMOS H_{160} band image for our J_{110} dropout selection. Our photometry is then conducted on our ACS, WFPC2, and NICMOS images, which are point-spread function matched to the NICMOS H_{160} image. Colors are measured in small-scalable (Kron 1980) apertures, assuming a Kron (1980) factor of 1.2. These fluxes are then corrected to total magnitudes using the light within a larger Kron (1980) aperture (adopting a Kron factor of 2.5). These latter corrections are made using the square root of the χ^2 image to improve the S/N. Figure 5 of Coe et al. (2006) provides a graphical description of a similar multi-stage procedure for measuring colors and total magnitudes. Typical aperture diameters are $0.3''$ and $0.6''$ for color and total magnitude measurements, respectively.

(b) *Selection Criteria:* We use the same selection criteria for identifying star-forming galaxies at $z \gtrsim 7$ that we used in our previous work on the identification of such galaxies in field data sets like GOODS or the HUDF (e.g., Bouwens et al. 2008). Specifically, we require a z -dropout candidate to satisfy the criterion $((z_{850} - J_{110})_{AB} > 0.8) \wedge ((z_{850} - J_{110})_{AB} > 0.8 + 0.4(J_{110} - H_{160})_{AB})$ where \wedge represents the logical **AND** symbol. J -dropout candidates are expected to satisfy the criterion $(J_{110} - H_{160})_{AB} > 1.3$. In cases of a non-detection in the dropout band, we set the flux in the dropout band to be equal to the 1σ upper limit. We require each candidate to be completely undetected ($< 2\sigma$) in all passbands blueward of the dropout band. We also demand that each candidate be detected at 5.5σ in the H_{160} band in a $0.5''$ -diameter aperture to eliminate spurious sources.

Our selection criteria are modified slightly for clusters that do not have NICMOS imaging in both the J and H bands. For clusters with only J band imaging, we apply a $(z_{850} - J_{110})_{AB} > 1.0$ criterion to select $z \sim 7$ z -dropouts and for clusters with only H band imaging, we apply a $(z_{850} - H_{160})_{AB} > 1.2$ criterion to identify possible star-forming galaxies at $z \gtrsim 7$. Both criteria should be successful in identifying candidate $z \gtrsim 7$ galaxies (albeit with a higher contamination level than selections relying on both J and H data).

4. RESULTS

After careful application of our selection criteria to all 11 clusters under study here, we identify 4 z -dropout candidates and 1 J -dropout candidate. We also uncover a small number of candidates that appeared to be promising $z \gtrsim 7$ candidates (e.g., the candidates at 00:26:37.90, 17:09:10.4 or 00:26:35.11, 17:10:10.3 behind CL0024), but which show modest ($\sim 2\sigma$) detections in passbands blueward of z_{850} and therefore were excluded.

Postage stamps of the four candidate star-forming galaxies at $z \gtrsim 7$ are provided in Figure 2. Other properties are given in Table 2. Our candidate in Abell 1689

TABLE 2
 $z \gtrsim 7$ z , J -DROPOUT CANDIDATES.*

Object ID	R.A.	Dec	$0.6\mu - J_{110}$ ^a	$0.8\mu - J_{110}$ ^b	$z_{850} - J_{110}$	$J_{110} - H_{160}$	H_{160}
$z \sim 7$ z -dropouts							
A1689-zD1 ^c	13:11:29.73	-01:19:20.9	$>2.5^d$	$>2.5^d$	$>2.2^d$	0.6 ± 0.2	24.6 ± 0.1
A2390-zD1 ^e	21:53:34.09	17:41:41.1	$>1.7^d$	$>1.5^d$	1.1 ± 0.8	0.8 ± 0.2	25.2 ± 0.2
A2667-zD1 ^e	23:51:40.06	-26:05:13.8	$>0.9^d$	$>0.4^d$	$>1.2^d$	0.0 ± 0.3	26.1 ± 0.2
A2667-zD2 ^e	23:51:36.85	-26:05:21.4	—	—	0.9 ± 0.4	0.0 ± 0.3	25.6 ± 0.2
$z \sim 9$ J -dropouts							
A2390-JD1 ^{e,g}	21:53:34.12	17:41:44.2	$>1.2^{d,f}$	$>1.1^{d,f}$	$>1.3^{d,f}$	>1.9	26.0 ± 0.2^g

*For uniformity of our analysis, all of the $z \gtrsim 7$ candidates here are from our own $z \gtrsim 7$ z and J dropout searches in cluster fields and do not include independent search results.

^aThis colour corresponds to $r_{625} - J_{110}$ for Abell 1689, $V_{555} - J_{110}$ for Abell 2390, and $V_{606} - J_{110}$ for Abell 2667.

^bThis colour corresponds to $i_{775} - J_{110}$ for Abell 1689 and $I_{814} - J_{110}$ for Abell 2390 and Abell 2667.

^cA1689-zD1 is our most robust $z \gtrsim 7$ candidate and was previously presented in Bradley et al. (2008).

^dLower limits on the measured colors are 1σ limits.

^eNo deep optical data are available for the four candidates: A2390-zD1, A2667-zD1, A2667-zD2, and A2390-JD1 (see Table 1). We consider all four to be relatively weak $z \gtrsim 7$ z -dropout candidates.

^fThe colours tabulated here are relative to the H -band, not the J_{110} -band, and hence are $0.6\mu - H_{160}$, $0.8\mu - H_{160}$, and $z_{850} - H_{160}$.

^gWhile this source is formally a 5.5σ detection in our reductions (and using our photometric procedures), there is some chance it may still be spurious.

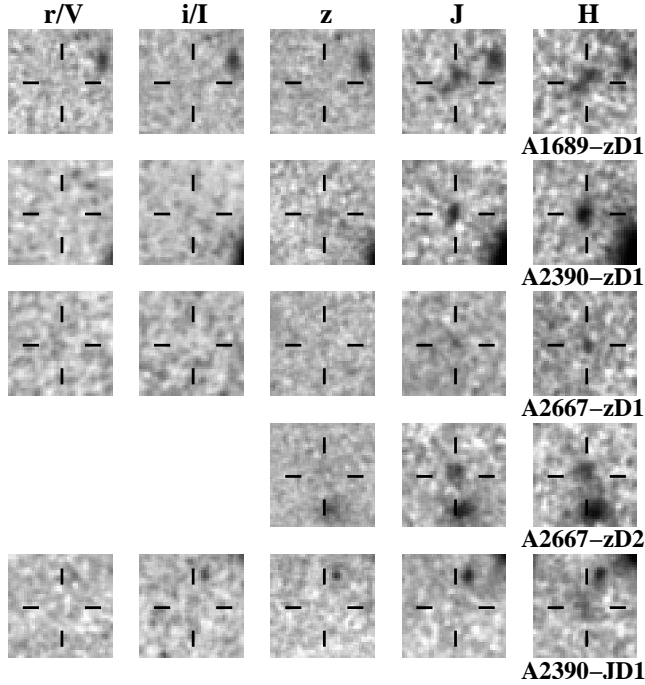


FIG. 2.— $r_{625}, i_{775}, z_{850}, J_{110}, H_{160}$ images ($4'' \times 4''$) of 4 $z \sim 7$ z -dropout candidates and one $z \sim 9$ J -dropout candidate (A2390-JD1), identified behind 11 massive lensing clusters. We consider the top source (A1689-zD1: Bradley et al. 2008) to be the only highly robust $z \gtrsim 7$ candidate in our cluster search fields. The leftmost two images correspond to the WFPC2 V_{555} and I_{814} bands for Abell 2390 and the WFPC2 V_{606} and I_{814} bands for Abell 2667. Deep WFPC2 data are not available for A2667-zD2.

has already been reported upon before by Bradley et al. (2008) and is by far the strongest candidate. The SED derived from the very deep optical, NICMOS, and IRAC data can only be successfully fit by the SED of a star-forming galaxy at $z \sim 7.6$ (Bradley et al. 2008).

Possible Contamination of our Selection by Lower-Redshift Galaxies: The four new sources in our selection are much less robust $z \gtrsim 7$ candidates. All are in clusters for which the optical data is much shallower.

The V_{555} , V_{606} , or I_{814} WFPC2 coverage over Abell 2390 and Abell 2667 reaches to only ~ 26.6 and ~ 26.5 (5σ , $0.3''$ -diameter aperture) over Abell 2390 and 2667, respectively. These WFPC2 data are ≥ 1 mag shallower than the ACS data available over 5 other clusters studied here (Table 1). This will result in a much higher contamination rate from low-redshift galaxies scattering into our color selection due to noise.

To estimate the expected contamination level, we start with a selection of intermediate magnitude galaxies in the HUDF NICMOS field (Thompson et al. 2005) and add noise to the fluxes to match the errors for sources in our search fields. On average, we find ~ 1 low-redshift contaminant over Abell 2390 and ~ 2 such sources over Abell 2667 in these simulations. This is comparable to the observed numbers and suggests that A2390-zD1, A2667-zD1, A2667-zD2, and A2390-JD1 may be low-redshift interlopers. As an alternate estimate of the contamination level, we start with the catalog of sources in the three clusters with the deepest ACS and NICMOS data (Abell 2218, MS1358, CL0024) and add noise (again to match the flux errors for sources behind Abell 2390 and Abell 2667). On average, we predict ~ 2 low-redshift contaminants over Abell 2390 and ~ 3.5 low-redshift contaminations over Abell 2667. Again these numbers are comparable to the observed number of candidates over these clusters and suggest that all four candidates behind these clusters may be interlopers. The modest differences in the predicted number of contaminants for the two methods is consistent with what one would expect from small number statistics.

Surface Density of Robust $z \gtrsim 7$ Candidates Behind Massive Galaxy Clusters: We tabulate the surface density of robust $z \gtrsim 7$ candidates found behind clusters as a function of magnitudes in Table 3. Also included in this table are the surface densities found in the field (Bouwens et al. 2008; R.J. Bouwens et al. 2008). The surface density of $z \gtrsim 7$ candidates behind clusters appears to be substantially larger than in the field at bright magnitudes (i.e., $H < 25.5$ or $> 5L^*$). This is exactly what we expect as a result of the slope of the LF at bright magni-

tudes. Interestingly, current observations do not provide any evidence for an enhancement in the surface density of $z \gtrsim 7$ sources between $H \sim 25.5$ and $H \sim 27.0$. This is despite the expected steep slope of the LF at such magnitudes. This could reflect the small numbers of sources involved here and point to the need for imaging more clusters to improve the overall statistics (see also §6 and R.J. Bouwens et al. 2008, in prep).

At $H \gtrsim 27$ AB mag we are probing faintward of L^* and likely reaching the regime where the effective slope of the LF is only moderately steep (i.e., $-d(\log \Phi)/d(\log L) \sim 0.7 < 1$: Bouwens et al. 2007). For such slopes, the trade-off between depth and area is such that the surface density of $z \gtrsim 7$ dropouts behind clusters will be lower than observed in the field.

5. DISCUSSION

5.1. Comparison with Model Expectations

We can compare the number of $z \gtrsim 7$ galaxy candidates found in our search with that expected based on determinations of the *UV* luminosity function (LF) at $z \sim 7$ from the field (Bouwens et al. 2008). For this calculation, we need lensing models for the clusters under study. We have such lensing models for 5 of the search clusters under study here, namely Abell 1689, Abell 1703, Abell 2218, CL0024, MS1358. These models are described in Limousin et al. (2007), Limousin et al. (2008), Elíasdóttir et al. (2007), Jee et al. (2007), and Franx et al. (1997), respectively. We will scale our expectations from those clusters to our entire sample.

Predicted Number of $z \gtrsim 7$ Candidates: Starting with the Bouwens et al. (2008) model for the sizes, *UV* colors, and *UV* LF for galaxies at $z \sim 7$ (Appendix B from that work), we generate very high-resolution mock images (pixel size $0.02''$) of galaxies in a $z \sim 7$ source plane and then remap these images to the image plane using available lensing models for these clusters. We then add these simulated fields to the real data and attempt to recover these sources using our cataloguing and selection procedures (§3). Generating these mock fields 20 times for each cluster and using our selection procedure to identify z and J dropouts, we estimate that we would expect to find 2.7 z dropouts over all of our search fields. If we repeat this procedure for $z \sim 8-10$ J -dropouts assuming an extrapolation of the Bouwens et al. (2008) LF results to $z \sim 9$, 0.3 J dropouts are expected. We find only modest variations in the number of dropouts expected behind clusters with similar depths and survey areas (e.g., ~ 0.2 predicted behind Abell 2218 vs. ~ 0.3 predicted behind MS1358). Similarly, use of slightly different lensing models for the clusters only appears to have a modest effect on the numbers (e.g., use of an updated version of the Broadhurst et al. 2005 model only increases the predicted numbers behind Abell 1689 by $\sim 20\%$ over that predicted by the Limousin et al. 2007 model).

Comparisons against the Number of Observed $z \gtrsim 7$ Candidates: The above predictions are quite consistent with the 1 robust z -dropout candidate, 3 other possible z -dropout candidates, and 1 possible J -dropout candidate discussed in §4, particularly given the small numbers and uncertain contamination levels. Because of the difficulty in interpreting the search results over the clusters with the shallower optical data (given the likely significant contamination levels), it also makes sense to restrict our

TABLE 3
SURFACE DENSITY OF STRONG $z \gtrsim 7$ CANDIDATES IN THE DEEP NEAR-IR DATA BEHIND CLUSTERS AND IN THE FIELD.

Location	Magnitude Range ^a	Surface Density (arcmin ⁻²)	Search Area per candidate (arcmin ²) ^b
Cluster	$H_{160} < 25.5$	$0.05^{+0.11}_{-0.04}$ ^c	21^{+101}_{-15}
Cluster	$25.5 < H_{160} < 26.5$	< 0.11 ^d	> 9
Cluster	$26.5 < H_{160} < 27.5$	— ^e	—
Field	$H_{160} < 25.5$	< 0.03 ^f	> 36
Field	$25.5 < H_{160} < 26.5$	$0.07^{+0.07}_{-0.04}$ ^f	13^{+16}_{-6}
Field	$26.5 < H_{160} < 27.5$	$0.48^{+0.38}_{-0.23}$ ^g	2^{+9}_{-1}

^aWithout any magnification from gravitational lensing and adopting the Bouwens et al. (2008) determination for L^* at $z \sim 7$, $H_{160} < 25.5$ corresponds to luminosities $> 5L^*_{z=7}$, $25.5 < H_{160} < 26.5$ corresponds to luminosities $> 2L^*_{z=7}$ and $< 5L^*_{z=7}$, and $26.5 < H_{160} < 27.5$ corresponds to luminosities $> 0.8L^*_{z=7}$ and $< 2L^*_{z=7}$.

^bThis column is the reciprocal of the previous column.

^cBased on the NICMOS data over all 11 galaxy cluster fields considered in this paper

^dBased on the NICMOS data over Abell 1835, Abell 2218, Abell 2219, Abell 2390, Abell 2667, MS1358, CL0024, and AC114

^eNear-IR data over cluster fields are not deep enough to probe this regime well. Nonetheless, we expect the surface density of $z \gtrsim 7$ dropouts behind clusters to be lower than observed in the field, since at $H \gtrsim 27$ AB mag we are probing faintward of L^* and likely reaching the regime where the effective slope of the LF is only moderately steep (i.e., $-d(\log \Phi)/d(\log L) \sim 0.7 < 1$: Bouwens et al. 2007). For such a slope, the trade-off between depth and area is such that the surface density of dropouts is lower behind clusters.

^fBased on the Bouwens et al. (2008) and R.J. Bouwens et al. (2008, in prep) search results for $z \gtrsim 7$ dropouts in the field. The R.J. Bouwens et al. (2008, in prep) search takes advantage of more than 20 arcmin² additional search area with NICMOS not considered by Bouwens et al. (2008).

^gBased on data from the HUDF Thompson field (Thompson et al. 2005), HUDF-NICPAR1, and HUDF-NICPAR2 fields (Bouwens et al. 2008)

comparison to only those clusters with the deepest data (i.e., excluding Abell 1835, Abell 2390, Abell 2667, and AC114 from this comparison). Using only clusters with the deepest optical data, we predict 2.0 $z \sim 7$ z -dropouts and 0.2 J -dropouts in total. Again this is in reasonable agreement with the 1 robust z -dropout we find over this more restricted search area, given the small number statistics. For both this comparison and the previous one, our search results are clearly consistent with our predictions and therefore with the Bouwens et al. (2008) $z \sim 7$ LF derived in the field. From this exercise, it is also quite clear that $z \gtrsim 7$ galaxy searches (using a small number of clusters) provide only a very weak constraint on the volume density of lower luminosity galaxies. For our search the uncertainty in the volume density of these sources is ~ 0.6 dex [factor of four] based on our sample size of one.

5.2. Comparison with Previous Results

Richard et al. (2006) reported finding 13 $z \gtrsim 6$ candidates (1st+2nd category) in ~ 12 arcmin² of ISAAC data behind 2 lensing clusters, while Richard et al. (2008) reported 12 other $z \gtrsim 7$ candidates in ~ 9 arcmin² of NICMOS data behind six other clusters.

The Richard et al. (2006) search results are significantly different from our results (13 $z \gtrsim 6$ candidates

TABLE 4

NUMBER OF STRONG $z \gtrsim 7$ CANDIDATES IDENTIFIED VS. THE NUMBER OF HST NICMOS ORBITS USED FOR THE SEARCH (SEE §6).

Location	# ^a	NICMOS Orbits	Candidates per Orbit	Orbits per Candidate ^b
Cluster (Shallow ^c) ^e	1	144	$0.007^{+0.016}_{-0.006}$	144^{+682}_{-101}
Cluster (Deep ^d) ^f	0	—	—	—
Field (Shallow ^c) ^g	3	~450	$0.007^{+0.007}_{-0.004}$	150^{+178}_{-74}
Field (Deep ^d) ^g	6	~600	$0.010^{+0.006}_{-0.004}$	100^{+65}_{-37}
Field (Both ^h)	9	~1050	$0.009^{+0.004}_{-0.003}$	117^{+56}_{-37}

^aNumber of strong $z \gtrsim 7$ candidates

^bReciprocal of the previous column

^cSearch results for shallow near-IR data with 5σ depths less than ~ 27 AB mag (i.e., ≤ 5 orbits). 27 AB mag corresponds to $\sim L^*$ at $z \sim 7$ (Bouwens et al. 2008).

^dSearch results for deep near-IR data, with 5σ depths greater than ~ 27 AB mag (i.e., ≥ 6 orbits). 27 AB mag corresponds to $\sim L^*$ at $z \sim 7$ (Bouwens et al. 2008).

^eAll 11 clusters considered here.

^fNo very deep (i.e., reaching > 27 AB mag at 5σ) near-IR data are available over clusters, but it is expected that the search efficiency will decrease significantly at fainter magnitudes since we will be probing faintward of L^* where the faint-end slope is likely only moderately steep (§6).

^gBased upon the NICMOS data considered in the Bouwens et al. (2008) and R.J. Bouwens et al. (2008, in prep) $z \gtrsim 7$ searches

^hSearch results for both shallow and deep near-IR data.

to $H_{160,AB} \sim 25$ over 12 arcmin² vs. the one robust candidate we find over 21 arcmin²). As we discuss in detail in Appendix C of Bouwens et al. (2008), $> 90\%$ of their $z \gtrsim 6$ candidates appear to be spurious, since none of the eleven $z \gtrsim 6$ candidates in their selection with substantially deeper (~ 1 -2 mag) NICMOS+IRAC coverage are significantly ($> 2\sigma$) detected.

The prevalence of $z \gtrsim 7$ galaxies implied by the Richard et al. (2008) search results is also much greater than what we find in our searches. Since these candidates are reported over a subset of the clusters used in the current search, the differences are puzzling. To understand the possible differences, we examined the Richard et al. (2008) sources in our own reductions of the same HST data using our photometric procedures. We find that 2 of their 12 candidates appear to be plausible $z \gtrsim 7$ galaxies given our photometry. The other sources are likely contaminants (a detailed discussion of all 12 Richard et al. 2008 candidates can be found in Appendix A). The two good candidates also satisfy our z -dropout selection criteria (but are blended with foreground galaxies in our search). One of these two $z \gtrsim 7$ candidates does not have particularly deep optical coverage, so there is a reasonable chance that it is at lower redshift.

A comparison of our $z \gtrsim 7$ sample with the Richard et al. (2008) $z \gtrsim 7$ sample suggests that our selection may suffer from some incompleteness. The observed level of incompleteness is not surprising and is consistent with what we expect from blending with foreground sources ($\sim 35\%$). Moreover, since this same incompleteness is implicitly included in the predictions we make in §5.1 to compare with the observations, the conclusions that we draw based upon those comparisons should be fair.¹

¹ Even if we include the two best $z \gtrsim 7$ candidates from the

6. IMPLICATIONS

The purpose of the present study is to increase the sample of candidate $z \sim 7$ galaxies and to assess the potential of gravitational lensing by galaxy clusters to identify and quantify the properties of galaxies at $z \gtrsim 7$. Lensing will increase the depth of the survey by the magnification factors, but decrease the search area by the same factor. If the effective slope of the LF ($-d(\log d\Phi)/d \log L$) is greater than 1, the gain in depth more than compensates for the loss in area, increasing the overall number of sources (e.g., Broadhurst et al. 1995). We would expect this effect to increase the numbers at bright magnitudes where the effective slope of the LF is very steep due to an apparent cut-off at the bright end (i.e., $H \lesssim 27$), but to decrease the numbers at fainter magnitudes ($H \gtrsim 27$) where the faint-end slope is shallower than this (i.e., $-d(\log d\Phi)/d \log L \sim 0.7 \lesssim 1$: e.g., Bouwens et al. 2007).

Our simulations (§5.1) show the expected gains at the bright end of the LF for searches behind clusters (see Table 4). We expect three $z \gtrsim 7$ galaxies over the present set of cluster data (144 NICMOS orbits) using the observed LF of Bouwens et al. (2008). The 48 NICMOS orbits/galaxy in the clusters for bright sources contrasts with the ~ 120 NICMOS orbits/galaxy needed in the field (nine $z \gtrsim 7$ galaxies are found in ~ 1050 orbits of NICMOS data over the GOODS fields: R.J. Bouwens et al. 2008, in prep). Nearly identical search procedures and selection criteria are used in both the cluster and field searches. Interestingly, the expected gains at bright magnitudes in clusters are not reflected in the observational results above, if we only include our most robust candidate (for ~ 144 NICMOS orbits/galaxy). This could easily arise because of small number statistics. Any gains in using clusters are likely to disappear at lower luminosities faintward of the LF knee, since the slope is not steep enough, as noted above.

Of course, lensing clusters can be used to potentially detect objects much fainter than in a field sample, thereby possibly extending the LF function to fainter limits. Unfortunately, both small number statistics and the challenges of modelling clusters make this very difficult, and likely not to be a very practical approach. This is because a substantial sample of objects is needed to faint limits to accurately determine the LF, as well as extremely accurate models of both lensing by the foreground cluster and incompleteness suffered by the lensed high-redshift population. Determining either of these latter two quantities well (and without any systematics) is a great challenge. As a result, it can be difficult to even measure quantities like the faint-end slope of the UV LF at $z \sim 4$, $z \sim 5$, and $z \sim 6$ from current samples of g , r , and i dropouts behind lensing clusters (where the samples are much larger: see R.J. Bouwens et al. 2008, in prep).

Our findings also underline the importance of having very deep optical data below the Lyman break for identifying high- z dropout galaxies. Without such data, it is essentially impossible to distinguish bona-fide $z \gtrsim 7$

Richard et al. (2008) selection in our sample, the total number of strong $z \gtrsim 7$ candidates is still very consistent with the predictions we make in §5.1 from the Bouwens et al. (2008) field LFs. Moreover, for the clusters with the deepest optical data (i.e., excluding AC114, Abell 1835, Abell 2390 and Abell 2667), only 2.2 $z \gtrsim 7$ candidates are predicted (§5.1) which is quite consistent with the 2 found (i.e., A1689-zD1 and A2219-z1).

galaxies from the large number of low-redshift galaxy interlopers that may scatter into $z \gtrsim 7$ samples as a result of noise – as we found for the four weaker $z \gtrsim 7$ dropout candidates in our selection (§4). Unfortunately, obtaining sufficiently deep optical data can be expensive and often requires $\gtrsim 2-3\times$ as much time as is spent obtaining the near-IR data.

We thank Richard Ellis, Marusa Bradač, Johan Richard, Daniel Schaerer, and Dan Stark for useful discussions. We thank Johan Richard for helping us to

more precisely locate some of his team’s lower S/N $z \gtrsim 7$ candidates in our own reductions of the available NICMOS data. We thank our referee for important feedback that was valuable for improving the overall clarity of our manuscript. This research used the facilities of the Canadian Astronomy Data Centre operated by the National Research Council of Canada with the support of the Canadian Space Agency. We acknowledge support from NASA grants HST-GO09803.05-A, HST-GO10874.04-A and NAG5-7697.

REFERENCES

- Bartelmann, M., Steinmetz, M., & Weiss, A. 1995, *A&A*, 297, 1
 Bertin, E. and Arnouts, S. 1996, *A&AS*, 117, 39
 Blakeslee, J. P., Anderson, K. R., Meurer, G. R., Benítez, N., & Magee, D. 2003a, *ASP Conf. Ser.* 295: *Astronomical Data Analysis Software and Systems XII*, 12, 257
 Bouwens, R. J., et al. 2004, *ApJ*, 616, L79
 Bouwens, R. J., & Illingworth, G. D. 2006, *Nature*, 443, 189
 Bouwens, R.J., Illingworth, G.D., Blakeslee, J.P., & Franx, M. 2006, *ApJ*, 653, 53
 Bouwens, R. J., Illingworth, G. D., Franx, M., & Ford, H. 2007, *ApJ*, 670, 928
 Bouwens, R.J., Illingworth, G.D., Franx, M., Ford, H. 2008, *ApJ*, in press, arXiv:0803.0548
 Bradley, L.D., et al. 2008, *ApJ*, 678, 647
 Broadhurst, T. J., Taylor, A. N., & Peacock, J. A. 1995, *ApJ*, 438, 49
 Broadhurst, T., et al. 2005, *ApJ*, 621, 53
 Coe, D., Benítez, N., Sánchez, S. F., Jee, M., Bouwens, R., & Ford, H. 2006, *AJ*, 132, 926
 Dunkley, J., et al. 2008, *ApJS*, submitted, arXiv:0803.0586
 Elíasdóttir, Á., et al. 2007, arXiv:0710.5636
 Franx, M., Illingworth, G. D., Kelson, D. D., van Dokkum, P. G., & Tran, K.-V. 1997, *ApJ*, 486, L75
 Jee, M. J., et al. 2007, *ApJ*, 661, 728
 Kron, R. G. 1980, *ApJS*, 43, 305
 Lehnert, M. D. & Bremer, M. 2003, *ApJ*, 593, 630
 Limousin, M., et al. 2007, *ApJ*, 668, 643
 Limousin, M., et al. 2008, arXiv:0802.4292
 Magee, D. K., Bouwens, R. J., & Illingworth, G. D. 2007, *Astronomical Data Analysis Software and Systems XVI*, 376, 261
 Meneghetti, M., Bartelmann, M., Jenkins, A., & Frenk, C. 2007, *MNRAS*, 381, 17
 Oesch, P. A., et al. 2008, *ApJ*, submitted, arXiv:0804.4874
 Oke, J. B., & Gunn, J. E. 1983, *ApJ*, 266, 713
 Richard, J., Pelló, R., Schaerer, D., Le Borgne, J.-F., & Kneib, J.-P. 2006, *A&A*, 456, 861
 Richard, J., Stark, D. P., Ellis, R. S., George, M. R., Egami, E., Kneib, J.-P., & Smith, G. P. 2008, *ApJ*, submitted, arXiv:0803.4391
 Stanway, E. R., McMahon, R. G., & Bunker, A. J. 2005, *MNRAS*, 359, 1184
 Szalay, A. S., Connolly, A. J., & Szokoly, G. P. 1999, *AJ*, 117, 68
 Thompson, R. I., et al. 2005, *AJ*, 130, 1

APPENDIX

A. INDEPENDENT ASSESSMENT OF THE $z \gtrsim 7$ CANDIDATES IN RICHARD ET AL. (2008)

Richard et al. (2008) also conducted a search for $z \gtrsim 7$ galaxy candidates behind 6 of the 11 galaxy clusters considered in this study (i.e., CL0024, CL1358, Abell 2218, Abell 2219, Abell 2390, Abell 2667). They reported finding 10 promising $z \sim 7$ z -dropout candidates and 2 promising $z \sim 9$ J -dropout candidates. Surprisingly, none of the 12 candidates in the Richard et al. (2008) $z \gtrsim 7$ sample make it into our own $z \gtrsim 7$ dropout selections (§4) – nor do our $z \gtrsim 7$ candidates appear in their selection – even though our color selection criteria are essentially identical (and their search data a subset of ours).

To understand the reason for these differences, we performed photometry on the sources using the same 0.3''-diameter (for ACS+WFPC2) and 0.6''-diameter (for NICMOS) apertures employed by Richard et al. (2008) for their photometry. We then corrected the magnitudes we measured from the ACS+WFPC2 or NICMOS data by 0.3 mag and 0.6 mag, respectively (again following the methodology of Richard et al. 2008). For the four Richard et al. (2008) candidates where light from the central cluster galaxy would contaminate the photometry (i.e., A2218-z2, A2390-z2, A2667-z2, A2667-j1), we explicitly fit the isophotes to the central galaxy and subtracted them off. A summary of our photometry of the 12 Richard et al. (2008) candidates is presented in Table A1. We present images of the 12 $z \gtrsim 7$ candidates from the Richard et al. (2008) selection in Figure 1.

Of the 12 candidates, two (i.e., A2219-z1 and A2667-z2) seem like plausible $z \gtrsim 7$ galaxies (A2219-z1 being the stronger of the two). Both candidates satisfy our selection criteria (but were blended with foreground galaxies in our catalogs and therefore not included in our candidate lists). The other ten candidates appear unlikely to correspond to high-redshift sources, given our photometry (although in the case of A2667-z1 it is difficult to rule out the source being at $z \gtrsim 7$). Ascertaining the precise redshift of A2667-z2 is difficult given the limited depth of the optical data around Abell 2667. Without deeper optical data, it is essentially impossible to know which $z \gtrsim 7$ candidates correspond to high-redshift galaxies and which are lower redshift contaminants. Note that we encountered similar difficulties in ascertaining the nature of the 4 weaker $z \gtrsim 7$ candidates found in our selection behind Abell 2390 and Abell 2667 (neither of which has particularly deep optical coverage). Our simulations and tests (§4) suggested that substantial contamination by low redshift galaxies is quite likely.

In addition to the above comments about specific $z \gtrsim 7$ candidates in the Richard et al. (2008) selection, we also have several general concerns about the properties of this z_{850} -dropout selection. Our first concern regards the $J_{110} - H_{160}$ color distribution of this selection. The colors are ~ 0.5 mag bluer on average than what we find in the field for our

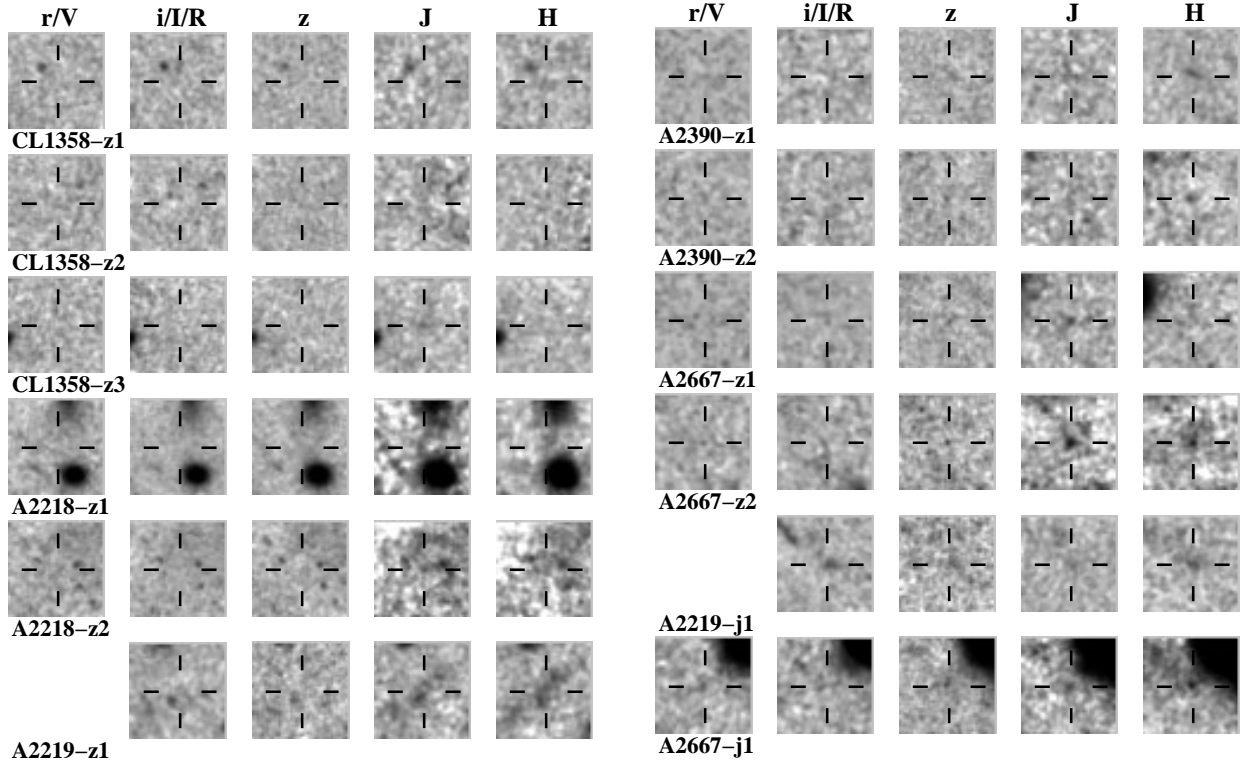


FIG. 1.— $r_{625}, i_{775}, z_{850}, J_{110}, H_{160}$ images ($4'' \times 4''$) of the 12 $z \gtrsim 7$ candidates in the Richard et al. (2008) selection. The images are scaled for display in the same way as we used in Figure 2 to present the $z \gtrsim 7$ candidates we identified behind clusters (and as used in presenting $z \gtrsim 7$ candidates in the HUDF/GOODS fields: Figure 3 from Bouwens et al. 2008). The leftmost two images correspond to the WFPC2 V_{555} and I_{814} bands for Abell 2390, the WFPC2 R_{702} band for Abell 2219, and the WFPC2 V_{606} and I_{814} bands for Abell 2667. Photometry for these candidates is presented in Table A1. A2219-z1 appears to be a blend of two sources, the upper right one of which appears to be a potential $z \gtrsim 7$ candidate. A2667-z2 satisfies our z -dropout selection criteria, but it is difficult to determine if it is a probable $z \gtrsim 7$ galaxy given the limited depth of the optical data (Table 1: see also §4). A2390-z1 and A2390-z2 have $z - J$ colours that appear to be too blue (see Table A1) for them to be $z \sim 7$ z -dropouts. The colors we measure for A2667-z1 do not satisfy our z -dropout selection criteria, but we cannot completely rule out this source as a $z \gtrsim 7$ candidate. CL1358-z1, CL1358-z2, and CL1358-z3 are not detected at $\geq 3\sigma$ significance in our reductions of the NICMOS data (the possible sources seen in the J -band data have a significance of only $1 - 2.7\sigma$ in our reductions). A2218-z1 is sufficiently close to a bright source, as to make unambiguous detection difficult. A2218-z2 is only found after subtracting the wings of the central cluster galaxy and is detected at only modest significance ($\sim 2 - 3\sigma$); the nature of this source is clearly very uncertain. Both A2219-j1 and A2667-j1 show significant detections at optical wavelengths and are almost certainly low redshift contaminants.

z -dropout sample (Bouwens et al. 2008: Figure A1). They are also ~ 0.5 mag bluer than what one would expect for a young $\beta = -2$ star-forming galaxy population (as observed at $z \sim 5 - 6$: e.g., Lehnert & Bremer 2003; Stanway et al. 2005; Bouwens et al. 2006). It is hard to understand why z -dropouts from the Richard et al. (2008) selection would be so much bluer than these expectations unless the candidates had strong $\text{Ly}\alpha$ emission in the J_{110} band. However, such an explanation would appear to be ruled out by the follow-up spectroscopy that Richard et al. (2008) conduct that find no such emission for the 7 z -dropout candidates they observe.

Second, we find it worrisome that almost all (8 out of 10) of their z_{850} -dropout candidates only satisfy their $z_{850} - J_{110}$ color criterion by a small margin (< 0.3 mag) whereas in the Bouwens et al. (2008) field sample, almost half of the z -dropouts satisfy the $z_{850} - J_{110}$ color criterion by a wide margin (i.e., > 1 mag). One would expect the situation to be quite opposite here, as a result of the much flatter number counts expected behind galaxy clusters (the number of bright sources in cluster fields would increase due to magnification by the cluster and the number of faint sources would decrease because of the loss of area). This should result in a *larger* fraction of sources satisfying the selection criterion by a wide margin, not a smaller fraction.

TABLE A1
INDEPENDENT PHOTOMETRY ON THE RICHARD ET AL. (2008) $z \gtrsim 7$ CANDIDATES.

Object ID	0.6''-diameter aperture ^a				
	$0.6\mu - J_{110}$ ^b	$0.8\mu - J_{110}$ ^c	$z_{850} - J_{110}$	J_{110}	H_{160}
$z \sim 7$ z -dropouts					
CL1358-z1 ^d	>1.9	>1.7	>0.8	27.6 ± 0.7	27.8 ± 0.7
CL1358-z2 ^d	—	—	—	>28.0	>28.1
CL1358-z3 ^d	>2.2	>2.0	>1.2	27.2 ± 0.4	>28.3
A2218-z1 ^{e,f}	2.0 ± 0.7	>1.8	>1.4	26.7 ± 0.2	27.6 ± 0.4
A2218-z2 ^e	0.9 ± 0.7	>0.9	0.5 ± 1.0	27.4 ± 0.5	26.9 ± 0.4
A2219-z1 (lower left) ^g	—	1.6 ± 0.2	0.5 ± 0.3	26.0 ± 0.2	26.0 ± 0.2
A2219-z1 (upper right) ^g	—	>3.0	1.0 ± 0.5	26.4 ± 0.3	26.3 ± 0.2
A2390-z1 ^h	>1.5	>1.6	0.0 ± 0.4	26.8 ± 0.3	26.6 ± 0.2
A2390-z2 ^h	>1.4	>1.3	-0.4 ± 0.7	27.4 ± 0.6	26.7 ± 0.3
A2667-z1 ^{f,i}	>2.1	>1.4	0.5 ± 0.4	26.6 ± 0.3	27.5 ± 0.6
A2667-z2 ⁱ	2.1 ± 0.7	>2.0	0.9 ± 0.3	25.6 ± 0.1	25.9 ± 0.1
$z \sim 9$ J -dropouts					
A2219-j1 ^j	—	2.0 ± 0.3^k	1.2 ± 0.5^k	26.7 ± 0.2	26.0 ± 0.2
A2667-j1 ^j	0.8 ± 0.4^k	>1.3 ^k	0.4 ± 0.4^k	27.8 ± 1.0	26.4 ± 0.2

^aFollowing the Richard et al. (2008) procedure, we have corrected the magnitudes we measure in a 0.3''-diameter and 0.6''-diameter aperture by 0.3 mag and 0.6 mag, respectively, for the WFPC2+ACS and NICMOS data (see Appendix A).

^bThis colour corresponds to $r_{625} - J_{110}$ for CL1358 and Abell 2218, $V_{555} - J_{110}$ for Abell 2390, and $V_{606} - J_{110}$ for Abell 2667.

^cThis colour corresponds to $i_{775} - J_{110}$ for CL1358 and Abell 2218, $R_{702} - J_{110}$ for Abell 2219, and $I_{814} - J_{110}$ for Abell 2390 and Abell 2667.

^dThese sources are not detected at high significance (i.e., $> 3\sigma$) in either the J_{110} or H_{160} bands in our NICMOS reductions. One possible reason that our calculated significance levels may be different from Richard et al. (2008) is that we account for sensitivity variations across the NIC3 detector in our weight maps (the sensitivities vary by factors of ~ 2 from region to region).

^eThese candidates lie close enough to bright sources, as to make unambiguous detection and robust measurement quite difficult.

^fThe measured $J_{110} - H_{160}$ color here is much bluer than those found for $z \sim 7$ galaxies in the field (Bouwens et al. 2008) – strongly suggesting this source is not a $z \sim 7$ galaxy.

^gA2219-z1 appears to be a blend of two sources (see Figure 1). While the lower left source is clearly a low redshift source, the upper right source seems to be a plausible $z \gtrsim 7$ candidate.

^hThe $z - J$ colours we measure for these sources appear too blue to correspond to dropout galaxies at $z > 7$.

ⁱThese candidates have colours that are consistent with those of galaxies at $z \sim 7$. However, it is difficult to be sure given the limited depth of the optical data over Abell 2667 (Table 1: §4).

^jThese sources are detected at $\geq 2\sigma$ at optical wavelengths in our reductions, strongly suggesting that they do not correspond to star-forming galaxies at $z > 7$. Richard et al. (2008) also note this fact and concede that these two sources are not particularly compelling $z \gtrsim 7$ candidates.

^kThe colours tabulated here are relative to the H -band, not the J_{110} -band, and hence are $0.6\mu - H_{160}$, $0.8\mu - H_{160}$, and $z_{850} - H_{160}$.